SENSITIVITY STUDY OF SONIC BOOM GROUND SIGNATURE USING DIFFERENT AXIAL DISTANCE STEP SIZES FOR EVALUATING NEAR-FIELD OVERPRESSURE

Jacques Gerard Tamayo [*1] **and Joana Rocha** [†1]
[1]Carleton University, Department of Mechanical and Aerospace Engineering

Abstract

To study the feasibility of supersonic commercial airliners, it is essential to better understand the impact of sonic boom caused by the aircraft. For simplicity, a general supersonic airliner concept by Sun et al. was used to conduct this analysis. Using an aircraft model created using Autodesk's Fusion 360 CAD program, the effects of the aircraft volume and lift in the near-field of the aircraft was determined using a custom MATLAB script developed in-house. The near-field overpressure was then propagated using NASA's PC Boom program to determine the ground signature of the airliner. Furthermore, a sensitivity analysis for the geometric and lift properties was conducted. It was determined that an axial step size of 1.2 m (i.e., the spacing between cross-sectional areas obtained from the 3D model used for the numerical differentiation) yields the best results for creating the full ground signature propagated by PC Boom, and that using this step size also results in better computation times compared to smaller step sizes. It was also observed that smaller step sizes for analysis caused noisier/unfiltered data in the F-Function curve which did not change the accuracy of the overall ground signature propagated by PC Boom. Finally, it was determined that a sufficiently large step-size causes the signature propagated by PC Boom to form a different shape compared to step-sizes less than 1.2 m, which should not be considered.

Keywords: Sonic boom, supersonic aircraft, sensitivity analysis

Résumé

Pour étudier la faisabilité d'avions commerciaux supersoniques, il est essentiel de mieux comprendre l'impact du bang sonique causé par l'avion. Afin de simplifier le problème, un concept général d'avion de ligne supersonique, proposé par Sun et al., a été utilisé pour mener cette analyse. Le modèle d'avion a été créé à l'aide du programme de CAO Fusion 360 d'Autodesk, les effets du volume et de la portance de l'avion dans le champ proche de l'avion ont été déterminés à partir d'un script MATLAB développé par les auteurs. La surpression en champ proche a ensuite été propagée à l'aide du programme ≪ PC Boom ≫ de la NASA pour déterminer la signature au sol de l'avion de ligne. De plus, une analyse de sensibilité pour les propriétés géométriques et de portance a été réalisé. Il a été déterminé qu'une taille de pas axial (c'est-à-dire l'espacement entre les sections transversales obtenues à partir du modèle 3D utilisé pour la différenciation numérique) de 1.2 m donne les meilleurs résultats pour créer la signature de sol complète propagée par PC Boom, et qu'en utilisant cette taille on obtient également de meilleurs temps de calcul, en comparaison à des tailles de pas axial plus petites. En outre, il a été observé que pour cette analyse, l'utilisation de tailles de inférieur à 1,2 m produisait des données plus bruyantes/non filtrées dans la courbe de fonction F, ce qui ne modifiait pas la précision de la signature globale du sol propagée par PC Boom. Enfin, il a été déterminé qu'une taille de pas suffisamment grande amène la signature propagée par PC Boom à former une forme différente par rapport aux tailles de pas inférieures à 1.2m, ce qui ne doit pas être pris en compte.

Mots clefs: Bang sonique, avions supersoniques, analyse de sensibilité

1 Introduction

Breaking the sound barrier by travelling faster than the local speed of sound will cause a sonic boom phenomenon, which typically results on a loud boom that can be heard from miles away. The sonic boom phenomenon cannot be avoided for aircraft travelling faster than the local speed of sound and the only way to mitigate the impact of the boom is to minimize the sonic boom which is caused by the aircraft. The sonic boom phenomenon is still a major challenge for modern day engineers designing supersonic aircraft designed to deliver passengers over long distances, in a shorter period of time compared to modern day commercial aircraft.

Minimizing the sonic boom produced by an aircraft were previously researched. For example, the X59 demonstrator aircraft by NASA and Lockheed Martin aims to produce a sonic boom loudness of 75 perceived level loudness (PLdB) at ground level which is equivalent to hearing a car door slam across a street [1]. Mathias Wintzer et al. have conducted a shape optimization process of a conceptual low-boom demonstrator aircraft and achieved an almost 10 PLdB reduction in the sonic boom loudness from the baseline [2]. Scarselli et al. have applied Carlson's method for simplified calculation of sonic boom signatures and conducted an optimization for minimizing sonic boom in their research [3]. Further

∗. jacquestamayo@cmail.carleton.ca
†. Joana.Rocha@carleton.ca

design optimizations for aircraft minimizing the sonic boom loudness were conducted by Rallabhandi et al. where adjoint-based shape optimization to design new low-boom concept models [4]. For the feasibility of supersonic flights, Sun et al. have performed an overview for different supersonic business jet concepts (SSBJ) highlighting the potential issues in environment, aircraft design, sonic boom loudness and ground footprint, aerodynamic efficiencies, and more [5].

The aim of the current study is to investigate the sonic boom phenomenon using a recreated supersonic airliner concept model (SSA) by Sun et al. [6], using a CAD program along with the concept model for sensitivity studies to determine the optimized parameters that should be used for further investigating the sonic boom ground signature of the concept model. Results from this study will allow future work for design optimization and considerations for minimizing the sonic boom ground signature.

2 Method

2.1 Linearized Flow Pressure Field

To study how sonic boom propagates from a vehicle travelling at supersonic speeds, the linearized flow pressure field of the vehicle evaluated at the near-field is required. The linearized flow pressure field of a supersonic vehicle can be determined using the following equation [7] :

$$\delta p\left(\tau;\theta\right)=\frac{\gamma p_0 M^2}{\left(2\beta r\right)^{\frac{1}{2}}}F\left(\tau;\theta\right) \tag{1}$$

The linearized flow pressure field of a vehicle is proportional to the specific heat of air γ, the ambient pressure at the flight altitude p_o, the square of the Mach number of the vehicle M and the *F-Function* of the aircraft F while being inversely proportional to the square-root of two times $\beta=\sqrt{M^2-1}$ and the radial position r evaluated from the centre of the aircraft. The linearized flow pressure field is evaluated at $\tau=x-\beta r$, which is the equivalent axial position of the aircraft translated to a point on the Mach plane formed by the vehicle [6]. The parameter θ is the azimuth angle evaluated at the vehicle coordinate system [7]. The near-field overpressure, or $\frac{\delta p}{p_0}$, can be determined from equation (2), which is required for PC Boom to propagate the sonic boom of the aircraft at near-field to the far-field to determine the ground signature [7].

2.2 Whittam's F-Function

The *F-Function* depends on both the geometry and lift distribution of the aircraft and is evaluated at axial stations on the vehicle. The *F-Function* was first introduced by Whittam and the concept was extended for wing-body configurations by Walkden [7], being determined using the following equation :

$$F\left(\tau;\theta\right)=\frac{1}{2\pi}\int_0^{\tau}\frac{A_e''\left(x;\theta\right)}{\sqrt{\tau-x}}dx \tag{2}$$

In equation (2), τ is the axial position of the vehicle translated to a position in the Mach plane, x is the axial position of the aircraft, and $A_e''(x)$ is the geometric second derivative of the equivalent area of the aircraft evaluated at an axial position [6]. Please do note that the area function $A_e''(x)$ is a discrete/numerical function of area data obtained from the 3D model and was not determined analytically with a continuous function using splines or other methods. The equivalent area of an aircraft is defined by equation (4), and consists of two different parts which are the equivalent area due to volume $A_v(x)$ and the equivalent area due to lift $A_l(x)$ [7].

$$A_e\left(x;\theta\right)=A_v\left(x;\theta\right)+A_l\left(x;\theta\right) \tag{3}$$

To calculate the F-Function at any given position τ, axial distance values x were used such that $x>\beta r$ to avoid singularity at $x=\tau$ and undefined integrals at $x<\beta r$.

2.2.1. Equivalent Area Due to Volume

The equivalent area of the aircraft due to volume $A_v(x)$ is the volume of air displaced by the aircraft as it travels through supersonic speeds and is defined as the cross-sectional area of the vehicle cut by the Mach plane tangent to a Mach cone which is projected to a normal axis in a given axial position x [7]. For axisymmetric slender bodies, the $A_v(x)$ is simply the normal cross-sectional area of the aircraft at a given axial distance [7].

2.2.2. Equivalent Area Due to Lift

The equivalent area of the aircraft due to lift $A_l(x)$ is determined using the lift distribution of the aircraft given axial distance and is determined using the following equation [6].

$$A_l\left(x;\theta\right)=\frac{\beta}{2q_\infty}\int_0^x L\left(x;\theta\right)dx \tag{4}$$

Here, $q_\infty=\frac{1}{2}\rho u^2$ is the dynamic pressure of the aircraft at the altitude with ρ as the density of air and u as the airspeed of the vehicle. The integral $\int_0^x L\left(x;\theta\right)dx$ represents the lift cumulative distribution of the aircraft where fully integrating the equation along the axis will give the total lift of the aircraft [7].

2.3 Aircraft Lift Approximation

The approximation of the lift function follows the method outlined by Scarselli et al. to determine the equivalent area displaced by lift required by the F-Function [3].

At level flight, the total lift of the aircraft is equal to the weight of the aircraft at cruising conditions where $L=W=mg$. The general lift equation of an aircraft is defined by [8] :

$$L=\frac{1}{2}C_l\rho u^2 A \tag{5}$$

in which ρ is the density of air, u is the airspeed, A is the total wing planform area, and C_l is the lift coefficient of the aircraft. Using the level flight condition of $L=W$, the lift

coefficient of the aircraft can be determined as $C_l = \frac{2W}{\rho u^2 A}$. The lift of the aircraft at a given axial distance $L(x)$ $\left[\frac{N}{m}\right]$ required for the equivalent area due to lift can be determined using the known values of ρ, u, and C_l, as following :

$$L(x) = \frac{1}{2} C_l \rho u^2 b(x) \tag{6}$$

where $b(x)$ is the wingspan of the aircraft at an axial position. The total integral $\int_o^L b(x)dx$, in which L is the aircraft length, is the total planform area of the aircraft wing. Similarly, the total integral $\int_o^L L(x)dx$ is the total lift of the aircraft at level-flight condition.

2.4 Propagating Near-Field Signature to Far-Field

To propagate the near-field overpressure of the aircraft to the far-field for obtaining the sonic boom ground signature, NASA's PC Boom program for Windows (ver. 671) was used. The PC Boom program is a fully ray-traced sonic boom program developed by NASA that can calculate sonic boom footprints and shapes from flight vehicles which can compute various ground signature shapes from different near-field sonic boom signatures [7]. The simple F-Function mode (Mode FFUNC) in PC Boom was used to propagate the calculated near-field overpressure (dP/P) of the SSA model cruising at 55000 ft altitude to determine the ground signature of the SSA model.

2.5 Aircraft Parameters and Design

The aircraft designed for analysis follows the supersonic airliner concept model from a study by Sun et al. as the dimensions are readily available from the study and a 3D model can be recreated using a CAD program for further study [6].

The mass of the aircraft at cruise condition is approximated as 80% of the maximum take-off mass (MTOM). The wing gross area uses the total area obtained by the approximated $b(x)$ function of the aircraft for consistency.

Table 1: Supersonic Airline Concept Model [6]

Aircraft Mass [kg]	78400
Cruise Mass [kg]	62400
Planform Area [m^2]	244.3

2.6 Supersonic Airliner Concept Model Recreation

The supersonic airliner concept model was recreated through AutoCAD's Fusion 360 CAD program using the dimensions from the general geometry sketch of the supersonic airliner concept design by Sun et al. [6], as shown in Figures 1 and 2. One notable difference between the recreated and the general model is the airfoil profile for the wing and elevator. Since it was difficult to determine the airfoil profile used by the general model, an ideal supersonic airfoil using the biconvex model was assumed and used for aircraft wing used to recreated 3D model [9].

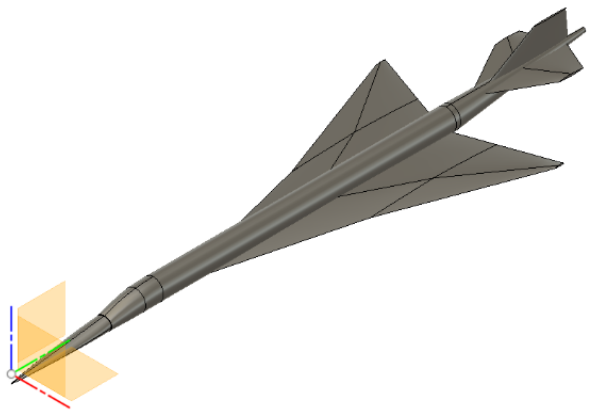

Figure 1: Recreated supersonic airliner (SSA) model in Fusion360 program

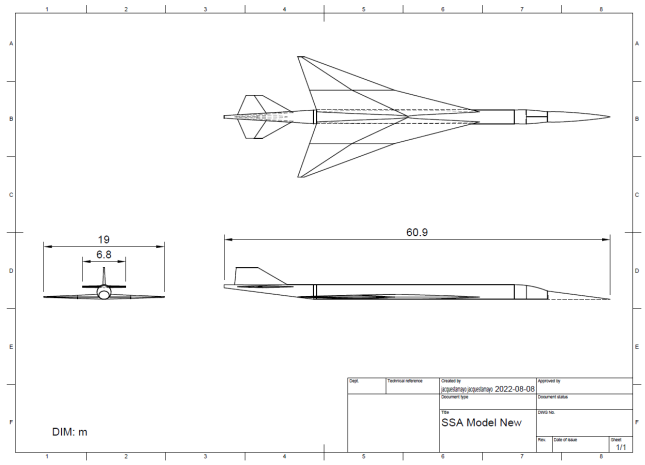

Figure 2: Three-view drawing of the recreated Supersonic Airliner (SSA) Model

2.7 Aircraft Flight Conditions

The aircraft flight conditions will follow the same conditions as the supersonic airliner concept model studied by Sun et al. [6], as shown in Table 2. The testing atmosphere uses the U.S. Standard Atmosphere model for temperature and humidity with no winds blowing at any given altitude. The air density, ambient pressure, and speed of sound at the given altitude were interpolated from charts available in fluid dynamics studies [10].

Table 2: Aircraft Flight Conditions [6]

Altitude (h) [m]	16764 (55000 ft)
Mach Number (M)	1.8
Air Density (ρ) [kg/m^3]	0.157
Air Pressure (p) [N/m^2]	1.371
Speed of Sound (v) [m/s]	295.1

3 Results

As mentioned in previous sections, the 3D model of the supersonic airliner concept was created using Autodesk's Fusion 360 CAD program. Fusion 360 was used to determine the cross-sectional area distribution of the aircraft given axial position. The F-Function and linear flow pressure field was calculated using MATLAB by creating an in-house MATLAB script, which was developed using the equations presented in the methods section. Lastly, the near-field overpressure calculated from MATLAB was used as an input for PC Boom, in order to propagate the sonic boom signature from the near-field to the far-field, to determine the ground signature of the sonic boom. The results for the aircraft geometry, F-Function, near-field overpressure, and propagated ground signature of the sonic boom uses an axial distance step size of 1.2 m for the results section. All step sizes of 0.2 m, 0.4 m, 0.6 m, 1.2 m, and 3.6 m were tested and results for the near-field overpressure, and propagated ground signatures were compiled on one plot for sensitivity analysis, as described in detail in the following sections.

3.1 Aircraft Geometry Functions

This section includes the volume distribution function of the SSA model (Figure 3), the wing geometry used (Figure 4), the area displaced by the lift (Figure 5), and the total area displaced by the SSA due to the volume and lift (Figure 5). The total wingspan of the aircraft is double the wing geometry function shown in the plot to include both sides of the wing.

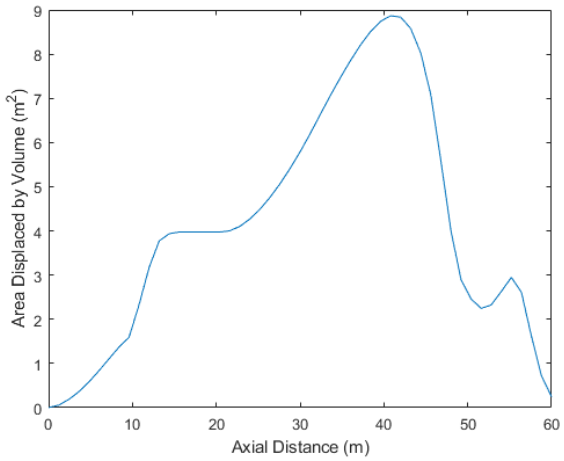

Figure 3: Cross-sectional area distribution of the SSA over axial distance (volume)

The cross-sectional area distribution function from Figure 3 follows the shape of the supersonic aircraft concept where an increase in cross-sectional area can be seen on both the wing section and the tail section, and the cross-sectional area distribution becomes constant after the nose section before the wing. The area displaced by lift uses the wingspan geometry from Figure 4 to form a cumulative distribution function (CDF) where the displaced area peaks at the downstream end of the wing. The total area function displayed on

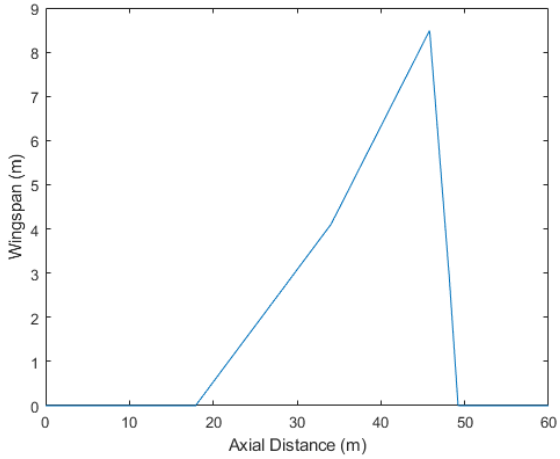

Figure 4: Wing geometry of the recreated SSA model for a single wing

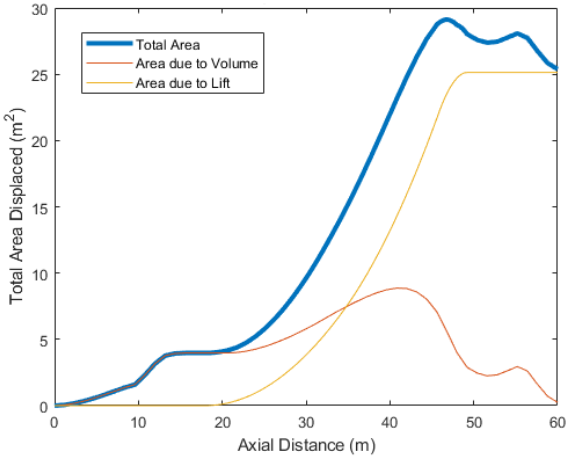

Figure 5: Total area displaced by the SSA due to volume and lift over axial distance

Figure 5 shows that the lift of the aircraft displaces air significantly more than the cross-section or volume of the aircraft and the combination of volume and lift greatly increases the area displaced by the aircraft. The cross-sectional area peaks formed by the wing and tail is more subtle in the total area displaced by the aircraft due to the area displaced by the lift.

3.2 Aircraft Geometry Derivatives

This section includes results for the second derivative functions for the area displaced by volume, the second derivative functions for the area displaced by lift, and the effects of both combined to find the total $A''(x)$ all seen on (Figure 6). Second order numerical differentiation methods, such as second order finite difference methods, were used on the MATLAB script to compute the derivative functions. All step sizes 0.2 m, 0.4 m, 0.6 m, 1.2 m, and 3.6 m were used to numerically differentiate the area functions $A(x)$ obtained from the supersonic airliner model to get the second derivative area functions $A''(x)$.

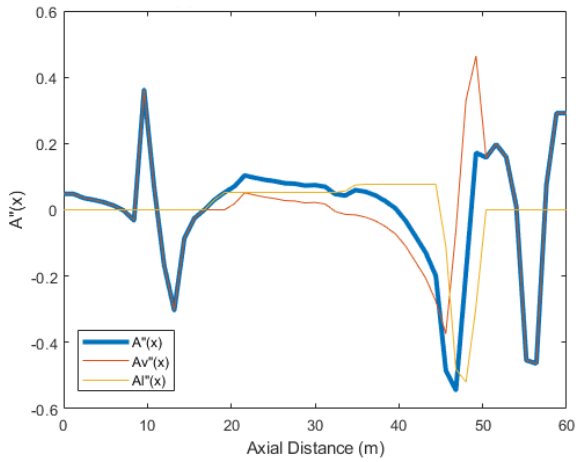

Figure 6: Total second derivative function of the SSA ($A''(x)$) combining area displaced by volume ($Av''(x)$) and lift ($Al''(x)$)

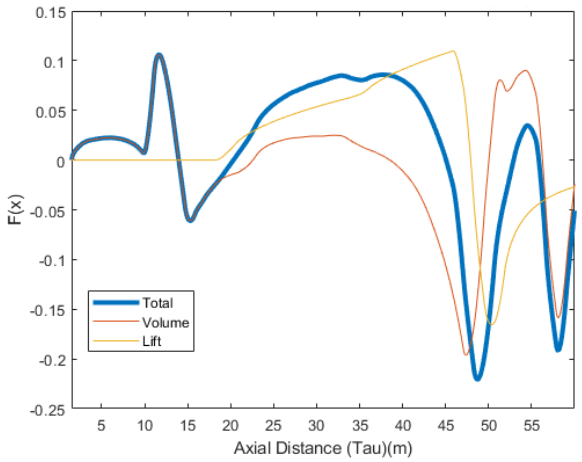

Figure 7: Total F-Function of the SSA model given axial distance compared with volume and lift F-Function

Due to the definition of Whittam's F-Function concerning the requirement of the second derivative of the total area of air displaced by the aircraft, the increase in magnitude of displaced area due to combining the lift contribution to volume is not enough to alter the linearized pressure field produced by the supersonic aircraft. The second derivative area function of air displaced by volume in Figure 6 shows increase in magnitude at places at the middle of the nose cone ($x = 10$ m) and downstream of the wing ($x = 50$ m) followed by a decrease in magnitude. The final increase occurs after the elevators ($x = 55$ m) in the tail. The second derivative area function of air displaced by lift in Figure 6 shows two visible constant lines followed by a sharp decrease downstream of the wing, and zero everywhere without the wing. This is because the wingspan distribution was determined using three different line equations.

Combining the second derivatives of the area displaced by the volume and lift shows that where the second derivative function of volume decreases in the wing section, the second derivative function of lift increases the magnitude in the wing section. This produces a balancing effect seen in Figure 6 where the total second derivative function $A''(x)$ positions itself near the zero magnitude line. One potential method for minimizing the sonic boom of the aircraft is to balance the second derivative of area displaced by volume and lift so the overall second derivative of displaced area have a magnitude that is close to zero.

3.3 F-Function Results

After determining the second derivative functions, one can calculate the F-Function due to the area displaced by both volume and lift (Figure 7). The F-Function due to volume and lift are then combined to find the total F-Function of the recreated SSA concept model (Figure 7). The numerical integration to find the F-Function was done by finding the Riemann sum of interpolated data points of $A''(x)$ with a fixed step size dx of 0.001 m for all test cases with axial step sizes of 0.2 m, 0.4 m, 0.6 m, 1.2 m, and 3.6 m.

The overall shape of the F-Functions for both volume, lift, and total F-Function in Figure 7 is greatly influenced by the shape of the second derivative functions of the area displaced by the aircraft where positive and negative peaks occur in the same places for the F-Function and the second derivative function. Similar to the second derivative function result, the F-Function due to volume and F-Function due to lift can cause a balancing effect in the wing section of the aircraft where a decrease in F-Function due to volume is increased by the increasing F-Function due to lift. It can be seen that total F-Function in Figure 7 decreases downstream of the wing due to the F-Functions due to lift and volume having a negative value, which is also observed for the second order area function. The F-Function due to lift is more effective in balancing the F-Function due to volume at the downstream end of the aircraft compared to the second derivative area function due to the F-Function due to lift having a non-zero and negative value.

3.4 Near-Field Overpressure

This section includes the linearized near-field pressure $\frac{\delta p}{p_0}$ calculated from the linearized flow pressure field equation using the total F-Function combining the volume and lift components, as shown in (Figure 8).

The near-field overpressure on Figure 8 simply follows the shape of the total F-Function of the aircraft with the magnitude being the only notable difference. Therefore, the trend in F-Function must be first examined to conduct a sonic boom minimization process. To minimize the sonic boom ground signature, the F-Functions due to lift and volume must first balance out the magnitude at the wing section and the F-Function due to lift must continuously decrease the F-Function due to volume at the downstream end of the aircraft. This conclusion is also supported by a research article by Sun et al. [6].

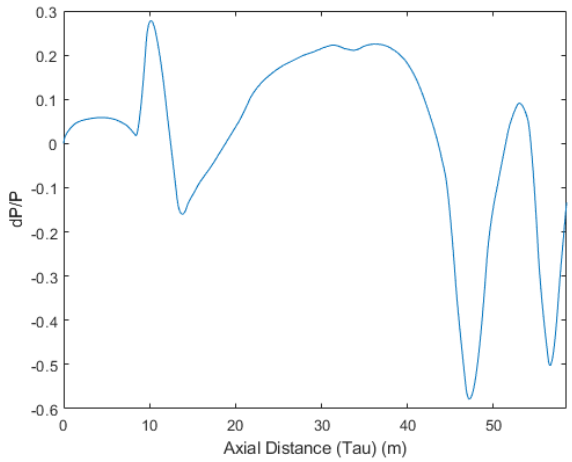

Figure 8: Near-field overpressure $\left(\frac{\delta P}{P_0}\right)$ of the SSA model given axial distance

3.5 Propagated Ground Signature

Once the linearized near-field pressure $\frac{\delta p}{p_0}$ has been calculated, it can be used as an input for PC Boom in order to obtain the propagated ground signature of the sonic boom. Results for the propagated sonic sound signature can be seen in (Figure 9).

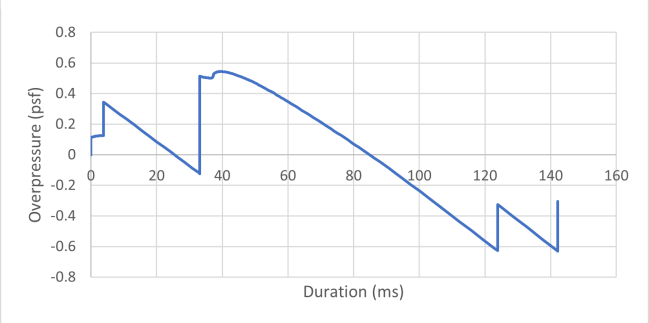

Figure 9: Sonic boom ground signature of the SSA propagated using PC Boom with near-field overpressure input (step size of 1.2 m)

3.6 Near-Field Overpressure (dP/P) Sensitivity Study

The combined results for the near-field overpressure calculated with MATLAB for all the axial step sizes used for sensitivity studies are determined (Figure 10). It is observed that the near-field pressure calculated for smaller step sizes have noisier data in-between and peaks have a higher amplitude for local minima and maxima.

3.7 Ground Signature Sensitivity Study

Finally, the combined results for the sonic boom ground signature propagated using PC Boom from the linearized near-field pressure calculated for all axial step sizes used are determined (Figure 11).

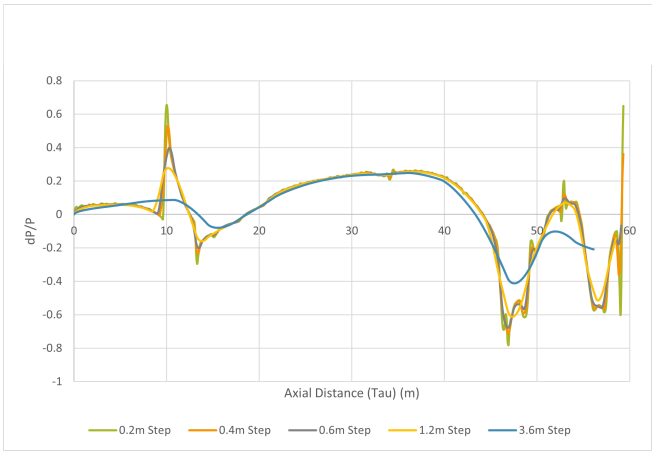

Figure 10: Near-field overpressure $\left(\frac{\delta P}{P_0}\right)$ of the SSA model given axial distance with all step sizes used

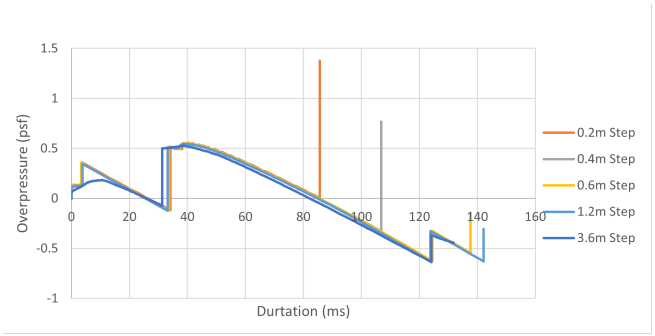

Figure 11: Sonic boom ground signature of the SSA propagated using PC Boom with near-field overpressure input with all step sizes used

3.8 MATLAB Calculation Run Time

The computation time for running the MATLAB script in order to calculate the F-Functions and linearized near-field pressure for the different axial step sizes are relatively inexpensive, as shown in (Figure 12) and Table 3.

Table 3: MATLAB computation time for all F-function and linear flow pressure field calculations with different step sizes

Step (m)	0.2	0.4	0.6	1.2	3.6
Computation (s)	164.28	106.20	86.53	65.68	47.00

4 Discussion

4.1 Near-Field Overpressure and Ground Signature Sensitivity Analysis

Different axial distance step sizes were tested to further understand how it affects the computation of the F-Function and the near-field overpressure of the aircraft. The numerical differentiation to get $A''(x)$ were done using the obtained data points for $A(x)$ and corresponding axial distance x from the Fusion 360 program.

It is observed in Figure 10 that smaller step sizes cause noisier in-between data to form and the peaks can have grea-

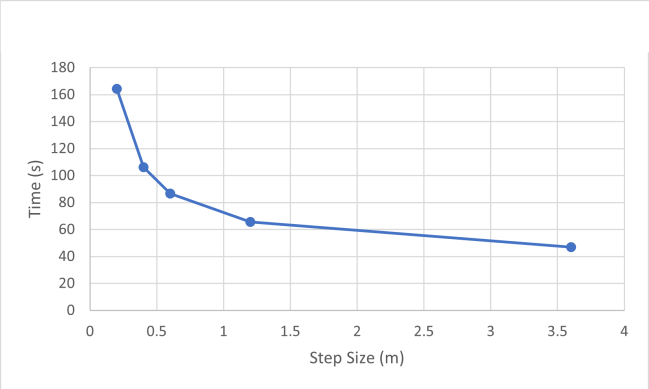

Figure 12: Plotted MATLAB computation time for all step sizes

ter magnitudes as seen at $x = 10$ m. More peaks can be observed for smaller step sizes due to noisier data as a result. It can be seen that the trend of the near-field overpressure for axial distance step sizes of 0.2 m, 0.4 m, 0.6 m, and 1.2 m are consistent in the locations for all the local positive maximum and negative minimum peaks with less noisy/unfiltered data in the near-field overpressure curve in case of the 1.2 m step size. The trend of the near-field overpressure, however, is inconsistent for the extreme case of using a 3.6 m step size where the near-field overpressure trend is only consistent at the wing area of the aircraft between $x = 15$ m to $x = 45$ m. The step size of 3.6 m is sufficiently large enough that the peaks observed in the trend have a much smaller amplitude and is overall inconsistent to the solution.

It is observed that the sonic boom ground signatures for step sizes 0.2 m, 0.4 m, 0.6 m, and 1.2 m have a consistent trend as seen on Figure 11. However, it was determined that PC Boom did not fully produce a complete ground signature for step sizes less than 0.6 m compared to the ground signatures produced using step sizes of 0.6 m and 1.2 m. The step size of 1.2 m shows the full sonic boom ground signature propagated over 142.158 ms while the step size of 0.2 m shows the ground signature ending at 85.692 ms. The step size of 0.6 m showed the second longest signature duration at 137.701 ms while a step size of 0.4 m has the second shortest duration at 106.837 ms. The extreme case of 3.6 m step size showed general consistency with the trend but the sonic boom overpressure shows different trend in the beginning and causes the earliest overpressure compared to other step sizes. The 3.6 m step size case has a sonic boom duration of 131.788 ms which is less than the 1.2 m step size case. Therefore, it is concluded that the step size of 1.2 m should yield the best result for determining the sonic boom ground signature propagated using PC Boom.

4.2 MATLAB Calculation Run Time

A MATLAB computation time analysis was done to further decide the optimal step size for repeat computations. It is observed in Figure 12 that the computation time trend is nonlinear and has diminishing returns for larger step sizes and exponentially longer times for smaller step sizes. Therefore, it can be concluded that the step size of around 1 m (1.2 m tested) is ideal for conducting repeat experiments for saving time in computing the necessary information such as the F-Functions and near-field overpressure using MATLAB.

5 Conclusions

In conclusion, it was determined that the optimal step size for repeat experiments using the MATLAB code and PC Boom for propagating near-field overpressure to producing sonic boom ground signature, is 1.2 m out of the other step sizes used for this test model case (supersonic airliner model). Using a 1.2 m step size will allow short computation times for MATLAB at 65.675 seconds, while producing a near-field overpressure and sonic boom ground signature that is consistent with smaller step sizes with less noisy/unfiltered data which did not change the accuracy and observable trend in the ground signature as propagated by PC Boom for this test case scenario. The shorter computation time and consistent results will allow more repeat experiments to be conducted in order to further study the sonic boom phenomenon.

Future works include testing different geometries for existing or concept aircraft vehicles, and attempting to minimize the sonic boom ground signature by designing an aircraft where the F-Function due to lift and volume can balance both the negative and positive peaks which can theoretically centre the F-Function near the zero-magnitude line.

Acknowledgments

The first author would like to thank Professor Joana Rocha for her supervision and support during the completion of this work.

References

[1] William Jeffrey Doebler and Jonathan Rathsam. How loud is x-59's shaped sonic boom? *Proceedings of Meetings on Acoustics*, 36, 2019.

[2] Mathias Wintzer, Irian Ordaz, and James W. Fenbert. Undertrack cfd-based shape optimization for a low-boom demonstrator concept. *33rd AIAA Applied Aerodynamics Conference*, AIAA 2015-2260, 2015.

[3] Gennaro Scarselli and Francesco Marulo. Sonic boom minimization through a simplified approach for the preliminary design of civil supersonic aircraft. *16th AIAA/CEAS Aeroacoustics Conference*, AIAA 2010-4006, 2010.

[4] Sriram K. Rallabhandi, Eric J. Nielsen, and Boris Diskin. Sonic-boom mitigation through aircraft design and adjoint methodology. *Journal of Aircraft*, 2014.

[5] Yicheng Sun and Howard Smith. Review and prospect of supersonic business jet design. *Elsevier Ltd.*, 2016.

[6] Yicheng Sun and Howard Smith. Conceptual design of sonic boom stealth supersonic transports. *CEAS Aeronautical Journal*, 13 :419–432, 2022.

[7] Juliet A. Page, Kenneth J. Plotkin, and Clif Wilmer. *PCBoom Version 6.6 Technical Reference and User Manual*. 2010.

[8] Daniel P. Raymer. *Aircraft Design : A Conceptual Approach*, volume 6. 2018.

[9] Jacob Siegler, Jie Ren, Leifur Leifsson, Slawomir Koziel, and Adrian Bekasiewicz. Supersonic airfoil shape optimization by variablefidelity models and manifold mapping. *Elsevier Ltd.*, 2016.

[10] Frank M. White. *Fluid Mechanics*, volume 8. 2016.